Mobility in epitaxial GaN: Limitations of free-electron concentration due to dislocations and compensation

M. N. Gurusinghe and T. G. Andersson
Applied Semiconductor Physics-MBE, Department of Microtechnology and Nanoscience, Chalmers University of Technology and Göteborg University, S-412 96, Göteborg, Sweden
(Received 28 October 2002; published 27 June 2003)

A detailed numerical description of the free-electron concentration and mobility due to charged dislocation lines is presented. The scattering at dislocations is numerically analyzed in addition to the other scattering mechanisms and the transverse mobility is calculated by the energy averaging technique. Furthermore, the effect on mobility from an unintentional bulk acceptor concentration is calculated at room temperature. Specifically the calculated mobility is presented as a function of the combined effect from free electrons (10^{15}–10^{19} cm^{-3}), dislocations (5×10^{8}–10^{12} cm^{-2}), and bulk acceptors (10^{15}–10^{19} cm^{-3}). Also compensation from 0 to 100% is considered. Results are compared with experimental mobility data. Most mobility results in epitaxially grown GaN layers intended for optical and electronic device structures are limited by $\sim10^{10}$ cm^{-2} dislocations and a compensation which is typically 30%–60%.

DOI: 10.1103/PhysRevB.67.235208 PACS number(s): 72.20.Jv, 61.72.Ss, 72.80.Ey

I. INTRODUCTION

Components of the group III nitride system and their ternary alloys are particular interesting due to their wide band gaps, which make them promising materials for optoelectronic and high-temperature electronic devices. Visible and UV light emitters,[1,2] blue lasers,[3] and UV detectors[4] are some examples. Recent progress in material growth and device fabrication has paved the way to produce high quality GaN-based heterostructure field-effect transistors[5,6] for high frequencies and power. The optimization of electronic devices based on GaN requires a detailed knowledge of the electronic properties of the epitaxial layers, especially concerning structural defects that are active and thus effecting charge carriers. The mobility and free-carrier concentrations are the key, easily measurable quantities that are important for device parameters. A good model which describes the electron scattering and the relation between doping, N_D, and free-electron concentration, n, based on the structural parameters is indispensable for the material and device physics as well as for the design of heterostructures and their devices.

In dislocation free bulk GaN the mobility at room temperature[7] is usually below 1000 cm^2/Vs for free-electron concentrations of 10^{16}–10^{18} cm^{-3}. Record values of 1245 cm^2/Vs at 5×10^{15} cm^{-3} have been reported.[8] Peak values[9] were 7386 cm^2/Vs for $n=2\times10^{15}$ cm^{-3} at 48 K. Most GaN material has native unintentional doping. This n-type conductivity may have its origin in N vacancies[10] or impurities such as silicon or oxygen.[11] The resulting energy position of such native defects and substitutional impurities have been calculated.[12,13]

Most GaN material used for devices is epitaxially grown. The main epitaxial techniques are metal organic vapor phase epitaxy (MOVPE), plasma-assisted nitrogen molecular beam epitaxy (MBE), or direct growth by MBE in ammonia. The lower growth temperature for MBE is a significant difference between MBE and MOVPE but it is not clear if this has any direct effect on free-carrier concentration or mobility. Sapphire (Al_2O_3) and silicon carbide (SiC) have proven to be important substrates because of the lack of lattice matched substrates. Layers grown on sapphire suffer from a biaxial strain due to the 14% lattice mismatch between GaN and sapphire(0001). This and the large difference in the thermal-expansion coefficient, 34% for the c-axis orientation, result in high concentrations of threading-edge and screw dislocations. On the atomic scale the lattice mismatch is balanced by inserted extra planes, which thus result in dislocation lines along the growth direction threading from the substrate-buffer interface to the surface.[14] On a nanometer scale the structure can be described as a columnar cell structure[15] where the columns are slightly tilted and/or misoriented (rotated) relative to each other thus providing a mosaiclike structure, whose details may be related to the growth. The effect on the final layer quality, and the mobility, has been studied for various growth parameters,[16] such as nitridation time,[17] substrate off-axis orientation,[18] buffer layers,[19,20] the III/V growth ratio,[21] and the type of nitrogen supply.[22] Much expertise has been gained but there is no conclusive picture.

In addition to the common scattering processes in semiconductors[23] and LO phonon, piezoelectric, and deformation-potential acoustic-phonon scattering, the dislocations give rise to an extra scattering term. Already in 1954, Reed published a statistical model for the charging of dislocations in germanium.[24] A few papers have analyzed the effect of scattering in bulk GaN in connection with dislocations.[25–28] Reed's model was used to describe the electron scattering in GaN due to negatively charged dislocation lines.[25] Furthermore, using Matthiessen's rule, the total drift mobility was calculated. The most pronounced effect of the dislocation density is to decrease the mobility with reduced free-carrier concentration.[25,26] It has even been suggested that the mobility may collapse due to the dislocations.[28] Moreover, in GaN layers there is often, at low temperatures, $T<30$ K, an apparent reduction in carrier concentration with temperature.[27] This has been interpretated by Look[27,29,30] and others[31,32] as an effect of a two-layer con-

duction where the second-layer conductivity takes place in the interfacial region at the substrate. A description of the temperature-dependent Hall-effect data has been made by solving the Boltzmann transport equation.[27] However, the dislocation filling factor described by Reed[24] was not considered.

Also other conduction mechanisms have been reported in highly resistive GaN layers.[33] For a high concentration of nitrogen vacancies there is a limited contribution from the scattering,[34] as well as contributions from silicon[35] and oxygen[36] donors. Another limitation may be the As in GaN, since in many MBE systems there is an arsenic background due to previous growth of GaAs. The arsenic in GaN is incorporated on the N site under *n*-type conditions[37] and is, in this case, expected to contribute as a neutral impurity scatterer.

It has been shown that the dislocation line is negatively charged[38,39] and therefore acts as a line of Coulomb scattering centers for conduction electrons. Using first-principles calculations, Neugebauer and Van de Walle[11] suggested that a deep acceptor level, introduced by the Ga vacancy (V_{Ga}) (or related complexes), is responsible for the yellow luminescence. Recently Elsner *et al.*[38] performed local-density-functional calculations on defects trapped at threading-edge dislocations in GaN. They interpreted the above state as an oxygen complex, $[V_{\mathrm{Ga}}-(\mathrm{O_N})_i]^{(3-i)-}$ ($i=$ 0, 1, or 2), with a deep energy state 1.0–1.2 eV above the valence-band edge. Such acceptor states are localized along the dislocation lines.

In this paper we have used Reed's model[24] developed for dislocations in Ge and rearranged it for wurtzite GaN, to calculate the free-electron concentration and mobility with the *n*-doping, compensation, and dislocation concentrations as parameters. The paper is organized in the following way. In Sec. II the charge balance around the charged acceptor states along the dislocation lines is described. In the numerical calculation, a degenerate energy level, $E_T=2.19$ eV, associated with the dislocation, below the conduction-band minimum, was considered.[38] In calculating the drift and Hall mobilities, the energy averaging technique was used. The result is a strong effect on the free-carrier density not only from the doping density but also due to the dislocation density. In Sec. III we show the mobility calculations and in Sec. IV the experimental values of mobilities and free-carrier densities at room temperature are described with dislocation and acceptor concentrations as parameters.

II. CHARGE BALANCE AROUND A DISLOCATION LINE

The charged nature of the dislocation free is the dominating factor and will scatter any charge carriers traveling through the system. Due to the long-range effects of the Coulomb interaction, this effectively prevents direct interaction between the charge carriers and the localized geometrical disturbance at the dislocations (assuming the expanded lattice in itself does not scatter electrons or holes). The effect of such scattering is to reduce the mobility.

In *n*-type GaN, Ga vacancies (V_{Ga}) or Ga vacancy complexes with oxygen ($V_{\mathrm{Ga}}-\mathrm{O_N}$), along the dislocation line, have an acceptorlike nature due to the unpaired dangling bonds.[38] Therefore, the dislocation can be treated as a row of closely spaced acceptor centers. These sites will become filled by electrons, thus removing free electrons from the conduction band, and the dislocation line will be negatively charged. In general, all sites are not filled which is described by the filling factor, f. If l is the spacing between occupied sites the fraction of charged sites is $f=c/l$, where c is the lattice spacing along the GaN (0001) direction. The corresponding volume density of electrons which occupies these sites is $(f/c)N_{dis}$, where N_{dis} is the dislocation density. Therefore the bulk charge balance equation becomes $N_D^+ = n+N_A^-+f\cdot(N_{dis}/c)$, where N_D^+ is the volume doping density and N_A^- is the corresponding unintentional acceptor density. The negative charge in the dislocation line will be compensated by a cylindrical positive space-charge region, with radius R, around the dislocation. Considering the line charge neutrality condition per unit length in the vicinity of the dislocation line, R is defined by

$$\pi R^2(N_D^+-N_A^-)=\frac{1}{l}=\frac{f}{c}. \tag{1}$$

The free electrons, n are repelled from this space-charge region and thus do not contribute. We define a critical value of f as f_0 through the minimum acceptable radius of the space-charge cylinder that is given by the basal lattice constant a of GaN. Then the relation between f and f_0 can be written as $R=a(f/f_0)^{1/2}$. When the conduction-band electrons fill the empty, degenerate sites along the dislocation, the electrostatic energy of the system increases. The potential energy of these states rises and the total electrostatic energy increases until nothing is gained energywise by transferring further electrons from the conduction band to the dislocation.

In an approach to derive an analytical expression for the total electrostatic energy, three contributions were considered.[24] First, the electron-electron interaction energy per electron per length, E_e, at the dislocation line is

$$E_e=E_0 f\left[\ln\left(\frac{f}{2c}\right)+0.577\right], \tag{2}$$

where E_0 is the energy of nearest-neighbor electron-electron interaction at the dislocation line, $E_0=q^2/4\pi\varepsilon c$. The value 0.577 is the Euler's constant. The second contribution is the energy stored in the surrounding positive space-charge region.

In order to derive an expression for the interaction energy of the positive charge in the space-charge region we solved the Poisson's equation around the dislocation for $r\leqslant R$,

$$\frac{1}{r}\frac{d}{dr}\left(r\frac{dV}{dr}\right)=-\frac{e\rho_p}{\varepsilon}=-\frac{e(N_D^+-N_A^-)}{\varepsilon}, \tag{3}$$

which leads to $V(r\leqslant R)=(e\rho_p/4\varepsilon)(R_0^2-r^2)$, where R_0 is a constant of integration, which is determined by the continuity of the potential at $r=R$. Since for $r\geqslant R$ the potential is the same as if all charges were concentrated along the axis of the cylinder, it may be convenient to use the integral form of Gauss's law. In this case the potential is given by $V(r\geqslant R)$

$=(eR^2\rho_p/2\varepsilon)\ln(1/r)$. By equating these potentials at $r=R$ and using the relation $\rho_p R^2=f/\pi c$ the potential term becomes

$$V(r\leqslant R)=\frac{ef}{4\pi\varepsilon}\left[1-2\ln(R)-\frac{r^2}{R^2}\right]. \tag{4}$$

The total interaction energy for a site due to positive space charge, E_p, can be written as $E_p=(1/2)l\int_0^R e\rho_p V(r\leqslant R)\cdot 2\pi r dr$. Substituting the potential term from Eq. (4) and integrating, we get

$$E_p=E_0 f\left[\frac{1}{4}-\ln(R)\right]. \tag{5}$$

The third contribution is the interaction of electrons at the dislocation line and the positive space-charge region. The interaction energy of the positive space charge and electrons at the dislocation line (E_{pe}) equals the integral of $(1/2)e\rho_p V_e(r,z)$ with respect to both r and z. However, this energy should be equal to the interaction energy of electrons at the dislocation line with the positive space charge (E_{ep}) provided by the conservation of energy. The interaction energy of electrons and the positive space charge is $E_{ep}=-(1/2)eV(r=0)$. This energy is equal to the interaction energy of the positive charges and electrons. From Eq. (4) it is given by

$$E_{ep}=E_{pe}=-\frac{1}{2}E_0 f[1-2\ln(R)]. \tag{6}$$

The total electrostatic energy per site, $E_s=E_e+E_p+E_{ep}+E_{pe}$, is found from Eqs. (2), (5), and (6). It can be expressed as

$$E_s(f)=E_0 f\left[\frac{1}{2}\ln\left(\frac{a^2f^3}{c^2f_0}\right)-0.866\right]. \tag{7}$$

Electrostatic energy variation of the positive space charge as a function of the distance from the dislocation for $r\leqslant R$ is, using Eq. (4),

$$E_r(r\leqslant R)=E_0 f\left[1+2\ln\left(\frac{1}{R}\right)-\frac{r^2}{R^2}\right]. \tag{8}$$

At $r=R$ Eq. (8) gives a nonzero value, which may produce a discontinuous conduction band near the dislocation. This can be avoided by assuming zero potential at $r=R$ and the energy for $r>R$ as the conduction-band energy. The band bending due to these negatively charged dislocation lines is given by (see the inset in Fig. 1)

$$E_r(r)=E_0 f\left(1-\frac{r^2}{R^2}\right). \tag{9}$$

In this consideration the total electrostatic interaction energy is given by $E_s(f)=E_0 f[\ln(f/c)-0.866]$, which is a good approximation for a material with both high dislocation and doping densities.

Next we find a mathematical description to the above phenomenon by considering the formation energy per electron at a site. A degenerate energy level E_T is associated to the sites localized along the dislocation line. The level is assumed to be in the energy gap and $E_T<E_F$, where E_F is the Fermi energy. If a dislocation has q number of electrons out of p number of possible sites, then the number of ways of arranging q electrons among p sites are $p!/(p-q)!q!={}^pC_q$. The free energy per site can be written as[24]

$$f\cdot G(f)=f\cdot\left[E_T-E_F+E_s(f)-\frac{k_BT}{fp}\ln({}^pC_q)\right], \tag{10}$$

where T is absolute temperature and k_B is the Boltzmann constant. In the model we assumed that a site can have one electron. Now at statistical and thermal equilibrium this free energy should be minimized with respect to f, which in turn depends on all parameters that contribute to the line charge. Then by taking the derivative of Eq. (10) with respect to f, the fractional charge occupation in the dislocation, f, is given by the familiar Fermi distributionlike function

$$f=\frac{1}{1+\exp\left[\dfrac{E(f)-E_F}{kT}\right]}, \tag{11}$$

where $E(f)$ is an explicit function of f: $E(f)=E_T+\dfrac{d}{df}fE_s(f)$. The derivative of $E_s(f)$ can be calculated by Eq. (7). In a first approximation we disregard any unintentional acceptor doping and only consider filling the acceptor states along the dislocation line. The dislocation charge filling factor, f, is not an independent parameter but determined by all concentrations of which N_{dis} and space charge are

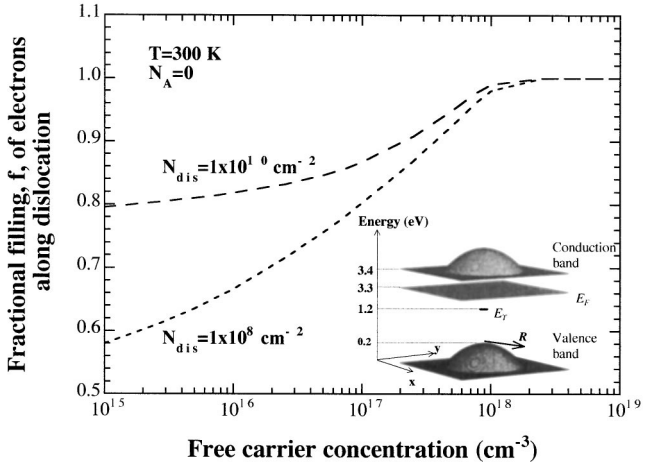

FIG. 1. Fractional filling of electrons along a dislocation line as a function of free-carrier concentration for two values of dislocation densities. The fractional filling increases the carrier concentrations and dislocation concentration. The inset illustrates the energy-band bending (not to scale) for $N_{dis}=1\times10^{10}$ cm^{-2}, $N_D=3\times10^{17}$ cm^{-3}, and $N_A=1\times10^{17}$ cm^{-3} due to a negatively charged dislocation line in n-type GaN. The radius of the cylindrical positive space-charge region depends on dislocation charge and the compensation in the material. Level E_T represents the localized energy state of the dislocation within the band gap.

important. With reference to Eq. (11), f is a function of free-electron concentration, n, through E_F and space charge $(N_D^+ - N_A^-)$ through f_0. The dislocation density dependence on f is from the bulk charge balance equation. The occupied fraction is small when the free-electron concentration, or dislocation density, is low as shown in Fig. 1. The probability of occupying the dislocation acceptor centers (sites) increases with both free-carrier concentration and dislocation density, respectively. At high carrier density, $n > 10^{18}$ cm^{-3}, or high dislocation density, $N_{dis} > 10^{10}$ cm^{-2}, almost all dislocation sites are occupied by electrons. As shown, the fractional occupation increases with dislocation density. The inset of Fig. 1 shows a calculated illustration of band bending due to the negatively charged dislocation line [using Eq. (9)] for $N_{dis} = 1 \times 10^{10}$ cm^{-2}, $N_D = 3 \times 10^{17}$ cm^{-3}, and $N_A = 1 \times 10^{17}$ cm^{-3}. As a result a $\sim$40 nm radius space-charge cylinder is formed around a dislocation line. Furthermore, the acceptance of electrons from conduction band to the dislocation lines will result in negatively charged dislocation lines. The effect on moveable electrons from these negatively charged lines is discussed in the next section.

III. MOBILITY DUE TO DISLOCATIONS

Any electrons moving near a negatively charged dislocation line will be scattered. This line charge acts as a Coulomb scattering center where the corresponding relaxation time has been analytically solved by Pödör,[40] considering a continuously charged negative line screened by ionized impurities and free electrons. The relaxation time for electrons moving perpendicular to a system of parallel dislocations is

$$\tau_{dis}(k) = \frac{\hbar^3 \varepsilon^2 c^2}{f^2 N_{dis} m^* e^4} \frac{(1 + 4\lambda^2 k_\perp^2)^{3/2}}{\lambda^4}. \tag{12}$$

The screening parameter λ is given by $\lambda = (\varepsilon k_B T / e^2 n')^{1/2}$. Here n' is the effective screening concentration, which may involve both free and bound carriers,

$$n' = n + (n + N_A^-)\left[1 - \frac{(n + N_A^-)}{N_D^+}\right]. \tag{13}$$

The wave vector normal to the dislocation line, $k_\perp$, is found by $E = (\hbar^2 / 2m^*) k_\perp^2$. The mobility component due to a time relaxation, e.g., from dislocation scattering, can be calculated by energy averaging,[41]

$$\frac{e\langle \tau_{dis} \rangle}{m^*} = \frac{4(k_B T)^{-5/2}}{3\pi^{1/2}} \frac{e}{m^*} \int_0^\infty \tau_{dis} E^{3/2} \exp\left(-\frac{E}{k_B T}\right) dE. \tag{14}$$

The numerically calculated mobility component from the dislocation scattering is shown in Fig. 2(a) as a function of the free-electron concentration. In general, according to Eq. (12), the dislocation mobility is inversely proportional to the $f^2 N_{dis}$. Since f depends on N_{dis} through the charge balance equation, the effect on the mobility cannot be seen explicitly but is illustrated by Figs. 1 and 2. Equations (7) and (11) were solved for f with a given free-carrier concentration, n, and dislocation density. The value of f was substituted into

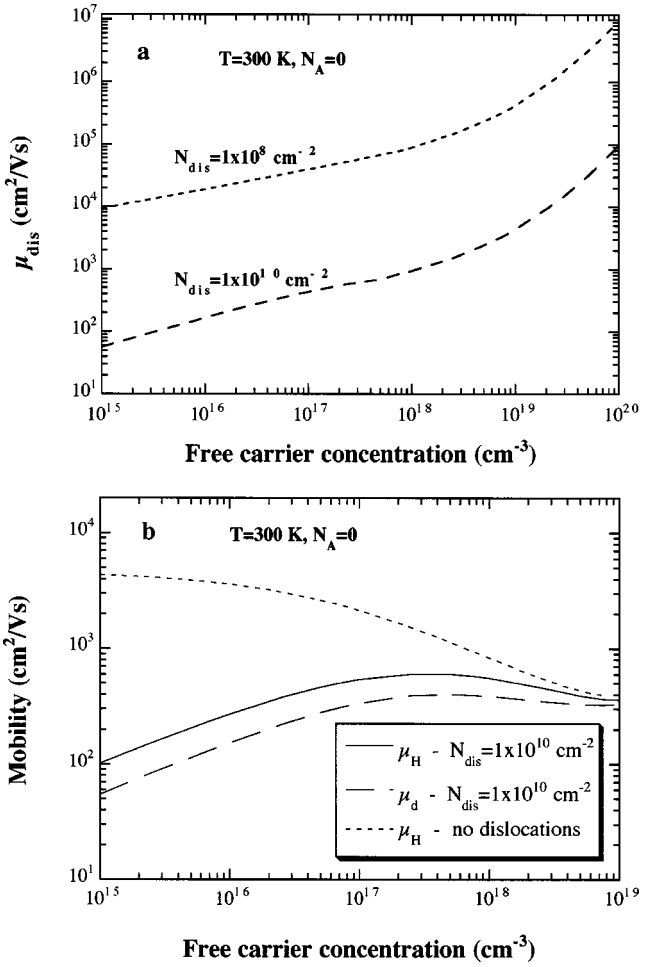

FIG. 2. (a) Calculated mobility component due to dislocation scattering as a function of free-carrier concentration. The mobility increases for reduced dislocations and increases linearly with free carriers lower than 10^{18} cm^{-3}. In the degenerate region it increases rapidly. (b) The calculated average transverse room-temperature mobility as a function of free-carrier concentration for GaN with $N_{dis} = 1 \times 10^{10}$ cm^{-2}. In the low carrier-concentration region the dislocations strongly reduce the mobility.

Eq. (14). Figure 2(a) clearly shows that the dislocation mobility decreases with reduced free-carrier density, which is opposite from the mobility in a pure and defect-free material. Since slope increases in the high carrier region, the scattering effect from the dislocations is strongly reduced. Consequently other scattering mechanisms dominate here. In the next section the effect of dislocations on the free-electron concentration and other parameters are presented for the dislocation densities 1×10^8 and 1×10^{10} cm^{-2}, i.e., in the typical range for GaN materials simply assuming zero acceptor concentration.

IV. TOTAL MOBILITY

In order to calculate the total average mobility, the other scattering mechanisms due to ionized impurities, acoustic phonons (deformation and piezoelectric), and polar optical phonons were added to the dislocation scattering. All of the

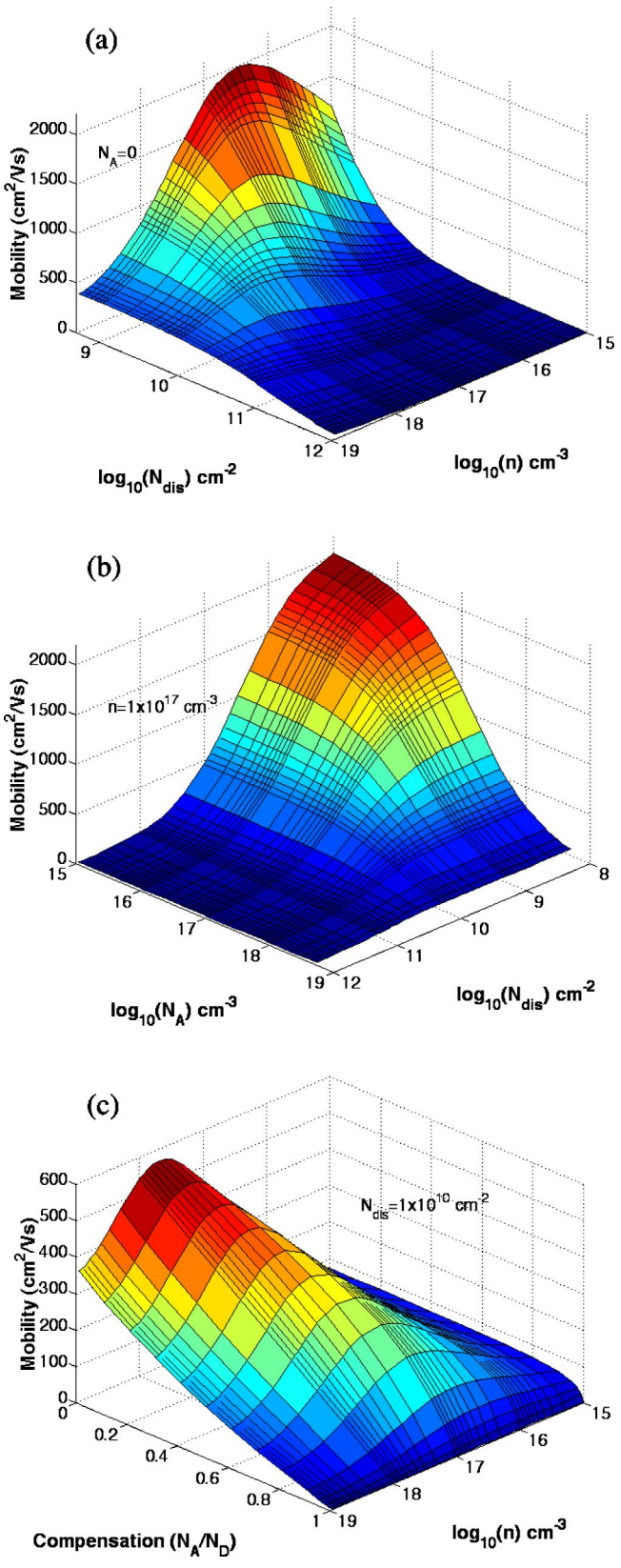

FIG. 3. Calculated transverse mobility as a function of (a) dislocation and free-electron concentrations for zero acceptor concentration, (b) dislocation and acceptor concentrations for 1×10^{17} cm^{-3} free electrons, and (c) free-electron concentration and compensation for 1×10^{10} dislocations/cm^2.

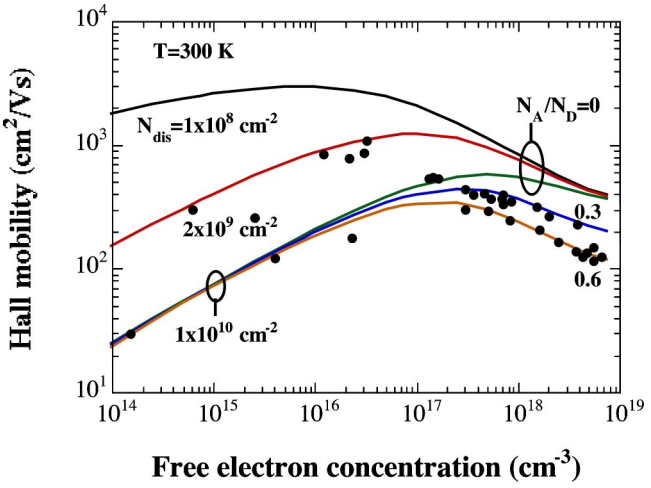

FIG. 4. Calculated (lines) and measured (symbols) Hall mobilities in GaN as a function of the free-electron concentration. Results from two sets of calculations are shown: variation of the dislocation density and 1×10^{10} cm^{-2} dislocation density with 0, 0.3, and 0.6 compensation ratios, respectively.

parameters needed were taken from Refs. 42 and 43. The numerically calculated drift mobility, μ_D, and Hall mobility, μ_H, are shown in Fig. 2(b). The Hall mobility is given by $\mu_H = e\langle\tau^2\rangle/m^*\langle\tau\rangle$. As a reference, the dotted line in Fig. 2(b) represents the calculated Hall mobility without any dislocations.

The mobility variation with free-electron concentration depends strongly not only on the dislocation density but also on doping and acceptor concentrations. In order to understand the relative importance of all parameters that govern the mobility, we calculated the dependency, a few parameters at a time, and illustrate this in a series of figures. First the net Hall mobility as a function of dislocations and free-carrier concentration for zero acceptors is shown in Fig. 3(a). For any value of the dislocation density, the mobility variation with carrier concentration has a maximum, which moves towards higher carrier concentration with increasing dislocation density. In general, increased dislocation concentration provides lower mobility while the mobility passes a maximum when varying the free electrons for a given dislocation density. By comparing an observed 300 K mobility of $\sim$1000 cm^2/Vs with our simulation, we conclude that such materials have a dislocation density of the order 10^{10} cm^{-2}.

Next we introduce the effect of unintentional acceptors. In Fig. 3(b) the mobility is shown as a function of dislocation and acceptor concentrations for a typical constant value, 1×10^{17} cm^{-3}, of free carriers. For high dislocation density the mobility is very low and independent of the acceptors. Also at a high concentration of acceptors the mobility is only slightly affected by the dislocations. To achieve high mobility the material should have low concentrations of both dislocations and acceptors. In Fig. 3(c) we show the mobility variation with compensation and free-carrier concentration for constant, 1×10^{10} cm^{-2}, dislocations. At zero compensation the highest mobility occurs for $4-5\times10^{17}$ cm^{-3} free carriers and the maximum mobility is reduced with compensation. Also that maximum is moved to the low carrier region with increasing compensation. Thus the overall effect of the

compensation is to reduce the mobility. Finally, in Fig. 4 we show the calculated Hall mobility for selected parameters which describe experimental data. The upper line represents an ultimate dislocation density since no such value has been found for GaN on sapphire. Increasing the density to 2×10^9 cm^{-2} describes very well the mobility with free-electron concentration, for best values around 1000 cm^2/Vs.[21] For higher electron concentration the mobility drops and the best description of experimental data is obtain only for $N_{dis}=1\times10^{10}$ cm^{-2} and after a compensation of 0.3 to 0.6 is introduced. In particular, much of the MOVPE data[20,44] and MBE data[22] can be modeled for 10^{10} cm^{-2} dislocations at a compensation ratio of 0.3–0.4. Many of the high mobility MBE-grown materials[26] tend to have a higher compensation of $\sim$0.6, which is in agreement with previous findings.[45]

The calculations clearly demonstrate the capability of the simplified model to describe the mobility in high defect density III nitrides. The model with a single dislocation line may be a generalization. In the complex structure with mosaiclike crystallites,[46] several dislocation lines are in close vicinity of each other. In such a dislocation cluster, each dislocation (or segment of dislocation) has a lower filling of electrons but is well represented by our model of a single line. Since both dislocation density and acceptor concentration strongly affect the mobility, one of them can be determined from calculations if the other parameter is measured.

V. CONCLUSION

We have investigated in detail the effect of dislocation charging on the electrical conduction in GaN. The free carriers are drained by the acceptor states along the dislocation line. The reduction in free-carrier concentration and the effect of mobility due to dislocation scattering were calculated. Special efforts were devoted to investigate the effect on mobility from the concentration of free electrons in the range 10^{15}–10^{19} cm^{-3} when the semiconductor contained a dislocation concentration in the range $\sim10^8$–10^{12} cm^{-2} and unintentional bulk acceptors (10^{15}–10^{19} cm^{-3}). Usually the mobility has a maximum depending on the above parameters. Calculated mobility values were compared to experimental data from GaN grown by MBE and MOVPE which provided values of dislocation density and acceptor concentration.

[1] H. Sakai, T. Koide, H. Suzuki, H. Yamaguchi, M. Yamasaki, S. Koike, M. Amano, and I. Akasaki, Jpn. J. Appl. Phys., Part 2 **34**, L1429 (1995).

[2] S. Nakamura, M. Senoh, N. Iwasa, and S. Nagahama, Appl. Phys. Lett. **67**, 1868 (1995).

[3] S. Nakamura, M. Senoh, S. Nagahama, N. Iwasa, T. Yamada, T. Matsushita, H. Kiyoku, and Y. Sugimoto, Jpn. J. Appl. Phys., Part 2 **35**, L74 (1996).

[4] M. Razeghi and A. Rogalski, J. Appl. Phys. **79**, 7433 (1996).

[5] M. A. Khan, M. S. Shur, J. N. Kuznia, Q. Chen, J. Burm, and W. Schaff, Appl. Phys. Lett. **66**, 1083 (1995).

[6] M. A. Khan, Q. Chen, J. W. Yang, M. S. Shur, B. T. Dermott, and J. A. Higgins, IEEE Electron Device Lett. **17**, 325 (1996).

[7] A. Saxler, D. Look, S. Elhamri, J. Sizelove, W. Mitchel, C. Sung, S. Park, and K. Lee, Appl. Phys. Lett. **78**(13), 1873 (2001).

[8] D. Look and J. Sizelove, Appl. Phys. Lett. **79**(8), 1133 (2001).

[9] D. Huang, F. Yun, M. Reshchikov, D. Wang, H. Markoc, D. Rode, L. Farina, C. Kurdak, K. Tsen, S. Park, and K. Lee, Solid-State Electron. **45**, 711 (2001).

[10] C. Wetzel, W. Walukiewicz, E. Haller, J. Ager, I. Grzegory, S. Porowski, and T. Suski, Phys. Rev. B **53**(3), 1322 (1996).

[11] J. Neugebauer and C. Van de Walle, Appl. Phys. Lett. **69**(4), 503 (1996).

[12] D. Jenkins and J. Dow, Phys. Rev. B **39**(5), 3317 (1989).

[13] I. Gorczyca, A. Svane, and N. Christensen, Solid State Commun. **101**(10), 747 (1997).

[14] B. Heying, X. H. Wu, S. Keller, Y. Li, D. Kapolnek, B. P. Keller, S. P. DenBaars, and J. S. Speck, Appl. Phys. Lett. **68**(5), 643 (1996).

[15] X. Du, Y. Wang, L. Cheng, G. Zhang, and H. Zhang, Mater. Sci. Eng., B **75**, 228 (2000).

[16] A. Hass, S. Zamir, O. Katz, B. Meyler, and J. Salzman, Mater. Sci. Eng., A **302**, 14 (2001).

[17] S. Davidsson, T. Andersson, and H. Zirath, Appl. Phys. Lett. **81**(4), 664 (2002).

[18] M. Fatemi, A. Wickenden, D. Koleske, M. Twigg, J. Freitas, R. Henry, and R. Gorman, Appl. Phys. Lett. **3**(5), 608 (1998).

[19] W. Fong, C. Zhu, B. Leung, and C. Surya, J. Cryst. Growth **233**, 431 (2001).

[20] C. Yang, M. Wu, C. Chang, and G. Chi, J. Appl. Phys. **85**(12), 8427 (1999).

[21] B. Heying, I. Smorchkova, C. Poblenz, C. Elsass, P. Fin, S. Den Baars, U. Mishra, and J. Speck, Appl. Phys. Lett. **77**(18), 2885 (2000).

[22] H. Tang and J. Webb, Appl. Phys. Lett. **74**(16), 2373 (1999).

[23] B. Ridley, B. Foutz, and L. Eastmann, Phys. Rev. B **61**(24), 16862 (2000).

[24] W. T. Reed, Philos. Mag. **45**, 775 (1954).

[25] N. G. Weimann, L. F. Eastman, D. Doppalapudi, H. M. Ng, and T. D. Moustakas, J. Appl. Phys. **83**(7), 3656 (1998).

[26] H. M. Ng, D. Doppalapudi, T. D. Moustakas, N. G. Weimann, and L. F. Eastman, Appl. Phys. Lett. **73**(6), 821 (1998).

[27] D. C. Look and J. R. Sizelove, Phys. Rev. Lett. **82**(6), 1237 (1999).

[28] J. L. Farvacque, Z. Bougrioua, and I. Moerman, Phys. Rev. B **63**, 115202 (2000).

[29] D. C. Look and R. Molnar, Appl. Phys. Lett. **70**(25), 3377 (1997).

[30] D. C. Look, J. Hoelscher, J. Brown, and G. Via, MRS Internet J. Nitride Semicond. Res. **6**, 10 (2001).

[31] D. Meister, M. Böhm, M. Topf, W. Kriegseis, W. Burkhardt, I. Dirnstorfer, S. Rösel, B. Frangis, B. Meyer, A. Hoffmann, H. Siegle, C. Thomsen, J. Christen, and F. Bertram, J. Appl. Phys. **88**(4), 1811 (2000).

[32] X. Xu, H. Liu, C. Shi, Y. Zhao, S. Fung, and C. Beling, J. Appl. Phys. **90**(12), 6130 (2001).
[33] P. Kordos, M. Morvic, J. Betko, J. Van Hove, A. Wowchak, and P. Chow, J. Appl. Phys. **88**(10), 5821 (2000).
[34] Q. Zhu and N. Sawaki, Appl. Phys. Lett. **76**(12), 1594 (2000).
[35] W. Götz and N. Johnson, Appl. Phys. Lett. **68**(22), 3144 (1996).
[36] R. Korotkov and B. Wessels, MRS Internet J. Nitride Semicond. Res. **5S1**, W3.80 (2000).
[37] C. Van de Walle and J. Neugebauer, Appl. Phys. Lett. **76**(8), 1009 (2000).
[38] J. Elsner, R. Jones, M. I. Heggie, P. K. Sitch, M. Haugk, T. Frauenheim, S. Öberg, and P. R. Briddon, Phys. Rev. B **58**, 12571 (1998).
[39] P. J. Hansen, Y. E. Strausser, A. N. Erikson, E. J. Tarsa, P. Kozodoy, E. G. Brazel, J. P. Ibbetson, U. Mishra, V. Narayanamurti, S. P. DenBaars, and J. S. Speck, Appl. Phys. Lett. **72**(18), 2247 (1998).
[40] B. Pödör, Phys. Status Solidi **16**, K167 (1966).
[41] D. C. Look, *Electrical Characterization of GaAs Materials and Devices* (Wiley, New York, 1989).
[42] D. C. Look, J. R. Sizelove, S. Keller, Y. Wu, U. Mishra, and S. DenBaars, Solid State Commun. **102**(4), 297 (1997).
[43] K. Shimada, T. Sota, and K. Suzuki, J. Appl. Phys. **84**(9), 4951 (1998).
[44] Z. Li, W. Lu, H. Ye, Z. Chen, X. Yuan, H. Dou, and S. Shen, J. Appl. Phys. **86**(5), 2691 (1999).
[45] J. Orton and C. Foxon, Semicond. Sci. Technol. **13**, 310 (1998).
[46] Y. Zhonghai, M. Johnson, T. Mcnulty, J. D. Brown, J. W. Cook, Jr., and J. F. Schetzina, MRS Internet J. Nitride Semicond. Res. **3**, 6 (1998).